A New Method To Determine *In Vivo* Interactomes Reveals Binding of the *Legionella pneumophila* Effector PieE to Multiple Rab GTPases

Aurélie Mousnier,[a*] Gunnar N. Schroeder,[a] Charlotte A. Stoneham,[a*] Ernest C. So,[a] James A. Garnett,[a,b] Lu Yu,[c] Steve J. Matthews,[a,b] Jyoti S. Choudhary,[c] Elizabeth L. Hartland,[d] Gad Frankel[a]

MRC Centre for Molecular Bacteriology and Infection[a] and Centre for Structural Biology,[b] Department of Life Sciences, Imperial College London, London, United Kingdom; Wellcome Trust Sanger Institute, Wellcome Trust Genome Campus, Hinxton, Cambridge, United Kingdom[c]; Department of Microbiology and Immunology, University of Melbourne, at the Peter Doherty Institute for Infection and Immunity, Melbourne, Victoria, Australia[d]

* Present address: Aurélie Mousnier, National Heart and Lung Institute (NHLI), Airway Disease Infection Section, Imperial College London, London, United Kingdom; Charlotte A. Stoneham, Department of Medicine, University of California San Diego, La Jolla, California, USA.

A.M. and G.N.S. contributed equally to this work.

ABSTRACT *Legionella pneumophila*, the causative agent of Legionnaires' disease, uses the Dot/Icm type IV secretion system (T4SS) to translocate more than 300 effectors into host cells, where they subvert host cell signaling. The function and host cell targets of most effectors remain unknown. PieE is a 69-kDa Dot/Icm effector containing three coiled-coil (CC) regions and 2 transmembrane (TM) helices followed by a fourth CC region. Here, we report that PieE dimerized by an interaction between CC3 and CC4. We found that ectopically expressed PieE localized to the endoplasmic reticulum (ER) and induced the formation of organized smooth ER, while following infection PieE localized to the *Legionella*-containing vacuole (LCV). To identify the physiological targets of PieE during infection, we established a new purification method for which we created an A549 cell line stably expressing the *Escherichia coli* biotin ligase BirA and infected the cells with *L. pneumophila* expressing PieE fused to a BirA-specific biotinylation site and a hexahistidine tag. Following tandem Ni^{2+} nitrilotriacetic acid (NTA) and streptavidin affinity chromatography, the effector-target complexes were analyzed by mass spectrometry. This revealed interactions of PieE with multiple host cell proteins, including the Rab GTPases 1a, 1b, 2a, 5c, 6a, 7, and 10. Binding of the Rab GTPases, which was validated by yeast two-hybrid binding assays, was mediated by the PieE CC1 and CC2. In summary, using a novel, highly specific strategy to purify effector complexes from infected cells, which is widely applicable to other pathogens, we identified PieE as a multidomain LCV protein with promiscuous Rab GTPase-binding capacity.

IMPORTANCE The respiratory pathogen *Legionella pneumophila* uses the Dot/Icm type IV secretion system to translocate more than 300 effector proteins into host cells. The function of most effectors in infection remains unknown. One of the bottlenecks for their characterization is the identification of target proteins. Frequently used *in vitro* approaches are not applicable to all effectors and suffer from high rates of false positives or missed interactions, as they are not performed in the context of an infection. Here, we determine key functional domains of the effector PieE and describe a new method to identify host cell targets under physiological infection conditions. Our approach, which is applicable to other pathogens, uncovered the interaction of PieE with several proteins involved in membrane trafficking, in particular Rab GTPases, revealing new details of the *Legionella* infection strategy and demonstrating the potential of this method to greatly advance our understanding of the molecular basis of infection.

Address correspondence to Gad Frankel, g.frankel@imperial.ac.uk.

*L*egionella pneumophila is a facultative intracellular pathogen, which infects protozoa and alveolar macrophages (1). Human infection can lead to a severe pneumonia, called Legionnaires' disease. Survival and replication of *L. pneumophila* in host cells rely on the ability to avoid degradation by the endolysosomal pathway (2). Instead, the bacteria remodel the phagosome into an endoplasmic reticulum (ER)-like, replication-permissive compartment, the *Legionella*-containing vacuole (LCV) (3, 4). Establishment of the LCV depends on the Dot (defective in organelle trafficking)/Icm (intracellular multiplication) type IV secretion system (T4SS), which translocates more than 300 effector proteins into host cells (5–8).

Dot/Icm effectors have been implicated in modulation of immune signaling, transcription, translation, and vesicular trafficking (9–11). Seminal work on the manipulation of the small GTPase Rab1 by seven effectors, SidM/DrrA, SidD, LepB, AnkX, Lem3, SidC, and LidA, revealed new enzymatic activities and highlighted the level of control that a pathogen can exert

over a host protein (reviewed in references 12 and 13). However, to date, activities or interaction partners have been described only for about 10% of the Dot/Icm effectors.

Studying the function of the Dot/Icm effectors is challenging due to their large number and functional redundancy. Conventional strategies to analyze the effect of single and multiple effector deletions on global phenotypes such as intracellular replication have remained largely unsuccessful. Instead, phenotypic analysis of single effectors expressed in host cells or heterologous systems such as yeast and approaches to identify their interaction partners are often the first choice. However, *in vitro* methods to identify interaction partners suffer from high rates of false positives and missed targets as they are performed out of the context of infection, in which numerous effectors disturb cellular homeostasis, resulting in the formation of noncanonical protein complexes and new and unique microenvironments such as the LCV.

The effector PieE, a 69-kDa protein, is conserved among *L. pneumophila* isolates and has two paralogs, PpeA/LegC3 and PpeB (14, 15). PieE deletion alone or with its paralogs did not affect intracellular replication, suggesting that it, together with effectors with redundant function, targets an important cellular process (14). *In vitro* experiments implicated PpeA in the manipulation of phagosome maturation (13); however, the host cell targets of PieE and its paralogs are still unknown. The aim of this study was to define the functional domains of PieE and, using a new tandem affinity (TA) purification procedure, to determine the PieE interactome under physiological infection conditions.

RESULTS

PieE is an integral LCV membrane protein exposing its Nt and Ct to the cytoplasm. Bioinformatic analysis of PieE predicts that it contains three coiled-coil (CC) regions upstream and one CC region downstream of two transmembrane (TM) helices (Fig. 1A). To test the domain prediction and localization of translocated PieE, A549 epithelial cells or THP-1 macrophages were infected with wild-type (WT) or $\Delta dotA$ (T4SS mutant) *L. pneumophila* 130b expressing PieE or PieEΔTM, lacking the putative TM helices, fused to four hemagglutinin (HA) tags. Immunofluorescence (IF) microscopy showed that PieE could be detected in infected cells as early as 1 h postinfection, and from 5 h, PieE surrounded most of the WT, but not the $\Delta dotA$, bacteria (Fig. 1B; see Fig. S1 in the supplemental material), indicating that PieE localizes to the LCV. This localization required the TM helices, as HA$_4$-PieEΔTM displayed a diffuse cytosolic distribution (Fig. 1B).

We next determined the topology of PieE in the LCV membrane. Infected cells were subjected to selective permeabilization with Triton X-100 or digitonin before immunostaining. Triton X-100 permeabilizes all cellular membranes and makes intracellular bacteria accessible for *Legionella* immunostaining (Fig. 1C, upper panels). In contrast, digitonin does not permeabilize the ER and the LCV (16), preventing immunostaining of bacteria in the LCV (Fig. 1C, lower panels). Importantly, in digitonin-permeabilized cells, the HA tag fused to the N terminus of PieE could be detected by IF microscopy (Fig. 1C, lower panels), demonstrating that it faces the cytosol. Together, the results indicate that the two predicted TM helices of PieE mediate its localization to the LCV membrane and that the N and C termini (Nt and Ct, respectively), containing the putative CC regions (CC1 to -4), are exposed to the cytosol (Fig. 1D).

PieE induces formation of regular arrays of stacked ER membranes. The lack of a replication defect of the *L. pneumophila* $\Delta pieE$ mutant (15) suggests that effectors with redundant function exist. We therefore investigated the functions of PieE and its predicted regions by transfection. In A549 (Fig. 2A) and HeLa cells (see Fig. S2A in the supplemental material), PieE localized to elongated, perinuclear structures. Deletion of the TM helices led to a diffuse cytoplasmic localization, suggesting that the PieE structures are formed of membranes. Deletion of each of the CC regions individually affected the morphology of the PieE-containing structures (Fig. 2A; see also Fig. S2A).

Costaining of PieE with markers of cellular membranes showed that calnexin, an integral protein of the ER, was partially redistributed into the PieE structures (Fig. 2B; also see Fig. S2B in the supplemental material), indicating that PieE aggregated or fused ER membranes. Furthermore, the rearrangement of the ER was accompanied by disruption of the Golgi apparatus (see Fig. S3A and B) and inhibition of trafficking of secreted alkaline phosphatase (SEAP) via the secretory pathway (Fig. S3C), showing that PieE interferes with the function of this pathway.

To determine the nature of the PieE-induced ER rearrangements, transfected HeLa cells were analyzed by transmission electron microscopy (TEM). In contrast to green fluorescent protein (GFP)-transfected control cells, which displayed normal ER ultrastructure, a significant subset of PieE-transfected cells contained striking accumulations of stacked membrane tubules in both longitudinal and transverse orientations (Fig. 3). The membranes of these tubules appeared to be tethered to one another at regular intervals. These coalesced tubules were continuous with both nuclear envelope (NE) and singular ER extensions. Cryo-immunoelectron microscopy confirmed that PieE and the ER marker protein disulfide isomerase (PDI) localized to the membrane arrays (see Fig. S5 in the supplemental material).

Similar ER structures were previously referred to as organized smooth ER (OSER) (17), which can be triggered by antiparallel dimerization of cytoplasmic domains of ER membrane proteins. We therefore investigated if PieE dimerizes by intermolecular CC region interactions using direct yeast two-hybrid (Y2H) assays. Coexpression of PieE fused to the GAL4 DNA-binding domain (DNA-BD) and the GAL4 transcription activation domain (GAL4 AD) rescued growth of yeast, showing that PieE can dimerize (Fig. 4A). Analysis of the role of PieE subdomains revealed that the N terminus (Nt) and C terminus (Ct), which contains CC4, interact (Fig. 4B). This conclusion is further supported by the observation that recombinant PieE Nt and Ct copurify as a complex. To validate an interaction between the N and C-terminal domains of PieE, we coexpressed a nontagged N-terminal domain construct (residues 1 to 426) with a His-tagged C-terminal construct (residues 476 to 555). Both the N- and C-terminal domains were pulled down after Ni-affinity chromatography, confirming a tight association between the two. Further analysis with size exclusion chromatography coupled with multiangle light scattering (SEC-MALS) revealed a 1:1 stoichiometry and, as expected, a molecular mass of 62 kDa of the complex (see Fig. S4 in the supplemental material). Mapping of the interacting regions implicated CC3 and CC4 but not CC1 or CC2 (Fig. 4B). Taken together, these data suggest that the different CC regions of PieE reorganize the reticular ER into regular, densely packed, membrane arrays and cause malfunction of the secretory pathway.
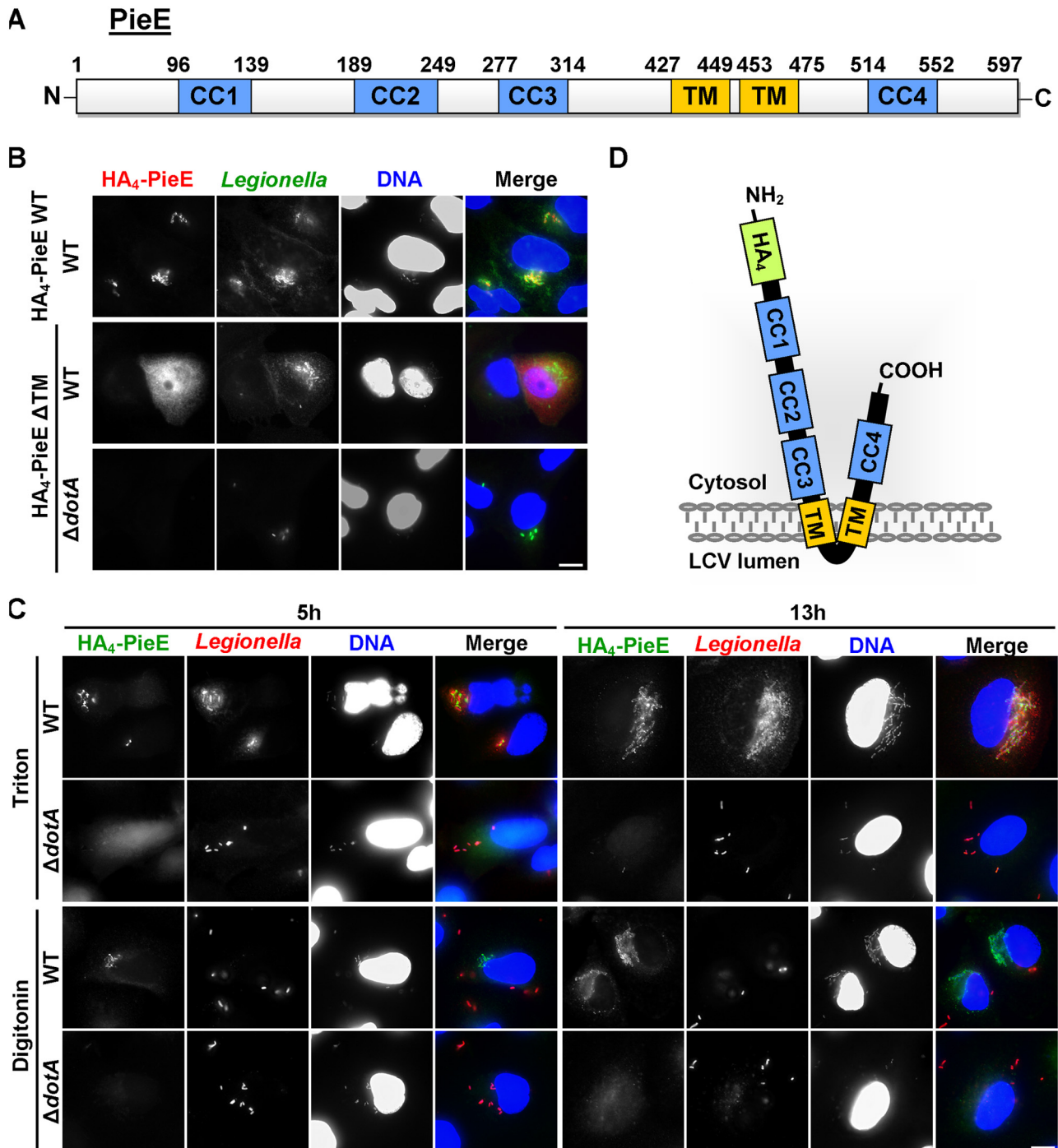
FIG 1 PieE inserts in the LCV membrane with its coiled-coil (CC) regions exposed to the cytoplasm. (A) PieE is predicted to contain 4 CC regions and two transmembrane (TM) helices. (B to D) PieE localizes to the LCV in a TM-dependent manner and exposes its CC regions to the cytoplasm. Fluorescent micrographs of A549 cells which were infected with *L. pneumophila* 130b WT or $\Delta dotA$ (T4SS mutant) expressing HA_4-PieE WT or ΔTM and processed for IF microscopy at 20 h postinfection (B) or fixed at 5 h or 13 h postinfection (C); permeabilized with Triton X-100 or digitonin, which, respectively, permeabilizes the LCV or not; and immunostained for *Legionella* and HA, allowing us to deduce the membrane topology of PieE (D). Bars, 10 μm.

The PieE *in vivo* interactome includes important regulators of membrane trafficking. To further dissect the function of PieE, we aimed to identify its host cell target proteins. However, as translocated PieE is a membrane protein found exclusively on the LCV, it is not amenable to conventional *in vitro* binding assays.

We therefore developed a new procedure for the isolation of binding partners from infected cells (scheme in Fig. 5). We created a plasmid for the expression of effectors with a His_6-Bio TA purification tag, consisting of a His_6 tag and a biotinylation site specific for the BirA biotin ligase from *Escherichia coli* (18, 19), and an
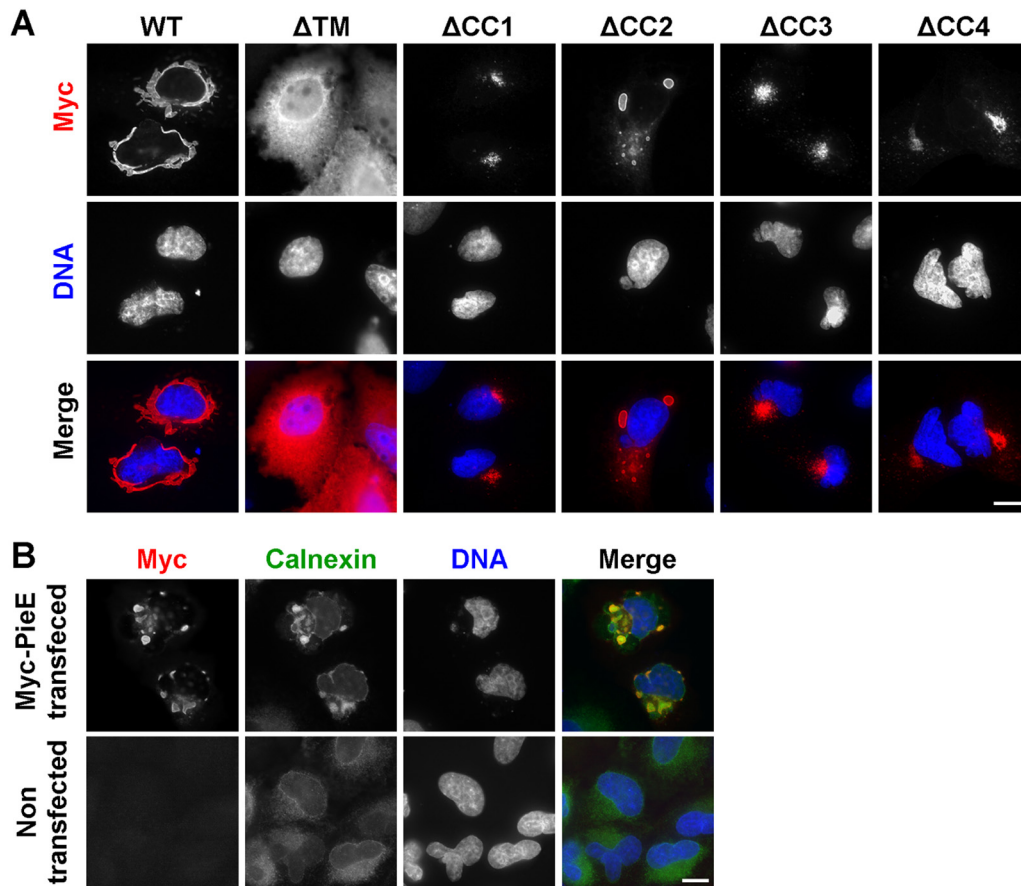
FIG 2 The CC regions of PieE induce reorganization of ER membranes. Myc-PieE was expressed in A549 cells, and its localization was analyzed by IF microscopy. (A) PieE localized to large, perinuclear structures, whereas PieEΔTM showed diffuse cytosolic localization. Upon deletion of individual CC regions (ΔCC1, -2, -3, or -4), PieE localized in each case to morphologically distinct structures. (B) Costaining showed that Myc-PieE redistributes and partially colocalizes with the ER marker calnexin. Bars, 10 μm.

A549 cell line stably expressing GFP-BirA. These cells were infected with *Legionella* 130b expressing His_6-Bio-PieE or His_6-Bio-LtpC, an unrelated effector (20), or 130b containing the empty vector as controls. Proteins were cross-linked *in vivo* with formaldehyde to preserve interactions, complexes containing the tagged effectors were purified under denaturing conditions by sequential Ni^{2+} nitrilotriacetic acid (NTA) and streptavidin affinity chromatography, and the isolated proteins were identified by liquid chromatography-tandem mass spectrometry (LC-MS/MS).

Analysis of the MS data using a *L. pneumophila* database revealed 34 unique PieE peptides (66.8% coverage) but no other *Legionella* proteins. Data analysis using the human IPI proteome database revealed, after elimination of hits also found in the control samples, 20 proteins which were specific for PieE (Table 1). Strikingly, several small GTPases, Rab1a, -1b, -2a, -5c, -6a, -7a, and -10 and Arf1/Arf3, were identified. Rab1a, -1b, -2a, and -6a and Arf1 are involved in vesicular transport between the ER and the Golgi apparatus, which is intercepted by *Legionella* to form the LCV (3) and is modulated by ectopically expressed PieE (Fig. 2). In addition, TFG, which is involved in protein secretion at the ER exit sites (21), and SCAMP3, which is a secretory carrier protein involved in trafficking in post-Golgi recycling and endosomal pathways (22), were identified. The PieE complexes also contained p62/SQSTM1, which plays a crucial role in selective autophagy, is recruited to LCVs in murine macrophages, and is implicated in inflammasome activation and restriction of bacterial growth, thus influencing the severity of disease (23, 24). Taken together, using this new method, we identified several proteins in the PieE interactome which were previously shown to be present on the LCV and implicated in LCV biogenesis or control of *L. pneumophila* infection.

PieE directly interacts with several Rab GTPases via CC1 and CC2. The TA purification technique does not discriminate between direct and indirect protein interactors. We therefore probed the interactions between Rab GTPases and PieE by Y2H assay. Coexpression of PieE with Rab1a, -1b, -2a, -5c, -6a, or -7, but not any of the proteins alone, restored growth of yeast on selective medium (Fig. 6, upper panel), indicating direct interactions. All the Rab GTPases, including Rab10, bound PieE Nt. Mapping of the Rab GTPase-binding region revealed a requirement of CC1 and CC2 but not CC3 for the interactions of all tested Rab GTPases with PieE Nt (Fig. 6, lower panel). These results validate the new TA purification method as a straightforward way to identify genuine effector targets during infection and demonstrate that CC1 and CC2 of PieE constitute a promiscuous Rab GTPase-binding site at the LCV.
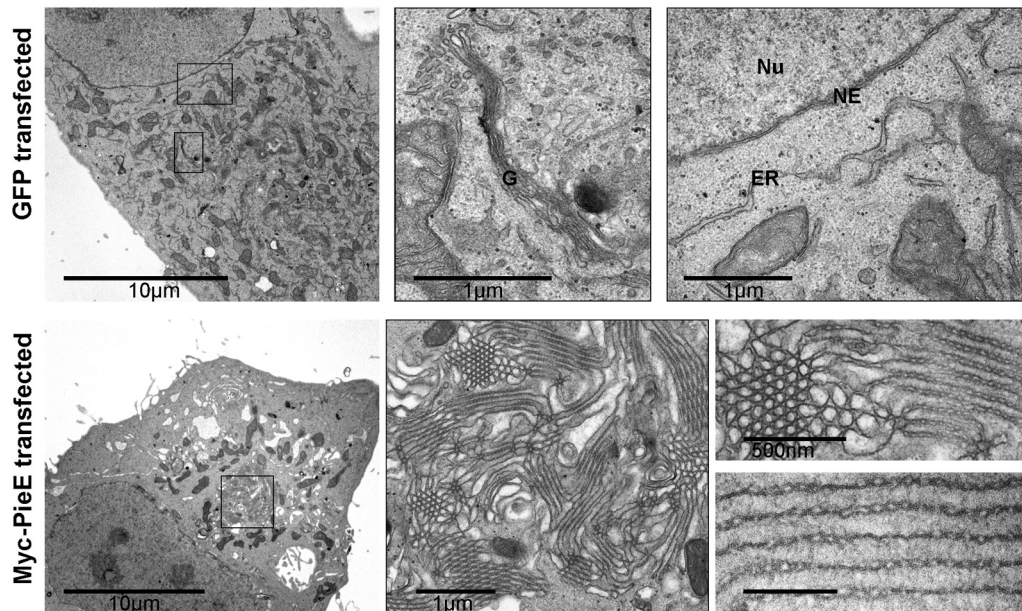
FIG 3 PieE induces organized smooth ER. PieE or GFP was expressed in HeLa cells for 24 h and processed for TEM, revealing unusual stacked tubular ER membranes in a significant subset of PieE-transfected cells. G, Golgi apparatus; ER, endoplasmic reticulum; Nu, nucleus; NE, nuclear envelope; PM, plasma membrane. Images are representative of two independent experiments.

DISCUSSION

The identification of functional domains and interaction partners is fundamental to understanding the role of proteins in cellular signaling. This is particularly challenging for translocated bacterial effectors, because infection often leads to substantial changes of the cellular proteome and, in the case of intravacuolar pathogens, formation of new organelles, which cannot be mimicked *in vitro*.

Here, we characterized the domains of the *L. pneumophila* effector PieE and used it as proof of principle to establish a new procedure to determine effector interactomes from infected cells. We uncovered that PieE localizes to the LCV and upon ectopic expression induces OSER by seemingly tethering tubules of ER together. Like other OSER-inducing proteins (17), PieE has the capacity to dimerize, which seems to be the main, but not exclusive, driver of ER remodeling. GFP-PieE was previously suggested to localize to the ER; however, ER rearrangements were not observed (15). As OSER formation also depends on rotational freedom of the dimerizing domains (17), this phenotypic difference is most likely due to steric hindrance inflicted by the GFP tag. In infection, membrane tethering by PieE could contribute to the flattening of vesicles around the LCV (25). Alternatively, PieE could facilitate the connection and fusion of LCVs in a superinfected cell, preventing biogenesis of several, individual LCVs.

Importantly, in order to gain insight in the function of PieE during infection, we engineered a novel TA purification method employing His_6 tag/Ni^{2+}-NTA and biotin/streptavidin purification steps, which, in combination with chemical cross-linking, allowed the isolation of protein complexes under highly stringent conditions. The ubiquitinated proteome of yeast and mammalian cells was previously analyzed by a similar strategy (19); however, this system used a 75-amino-acid biotinylation site from a *Propionibacterium shermanii* transcarboxylase, which is modified by various biotin ligases. By using the 15-residue BirA-specific biotinylation site (18) and providing BirA in the host cell, we minimized the length of the tag and included an additional level of specificity, as background due to effector remaining in bacteria is minimized.

Our method overcomes several limitations of *in vitro* approaches such as Y2H assays. As evidenced by PieE, which is a large membrane protein and insoluble when expressed in *E. coli* (data not shown), the expression of the bait effector in its natural background rather than heterologous systems reduces problems, such as cytotoxicity and poor solubility or stability, which obstruct the characterization of many effectors. Most importantly, our method avoids high rates of false positives or missed interactions which compromise *in vitro* approaches, as they do not account for the unique environment encountered in an infected cell. During infection, the global proteome of the host cell is altered as part of the host defense response but also due to the action of numerous effectors (9, 11, 26, 27). Organelles are also altered during infection, and although the LCV has ER-like characteristics, it was demonstrated that the LCV has a unique proteome (28, 29). Finally, as demonstrated for LubX and SidH (30), effectors can target each other instead of or in addition to host cell proteins.

Importantly, we found several Rab GTPases involved in vesicle traffic between the ER and the Golgi apparatus (Rab1a, -1b, -2a, and -6a) and in the endosomal system (-5c, -7a, and -10) in the PieE interactome. Although earlier studies indicated that Rab2, -5, -6, and -10 are not recruited to the LCV, they were recently found in the LCV proteome (28), confirming that they cocompartmentalize with PieE.

The cross-linking step of the TA method potentially allows the isolation of secondary interactors which do not directly bind the effector and stabilizes weak interactions. Using Y2H, we confirmed that all interactions of PieE with the isolated Rab GTPases were direct. This validated PieE as the first Dot/Icm effector which interacts with Rab2, -5, -7, and -10 during infection. However, a
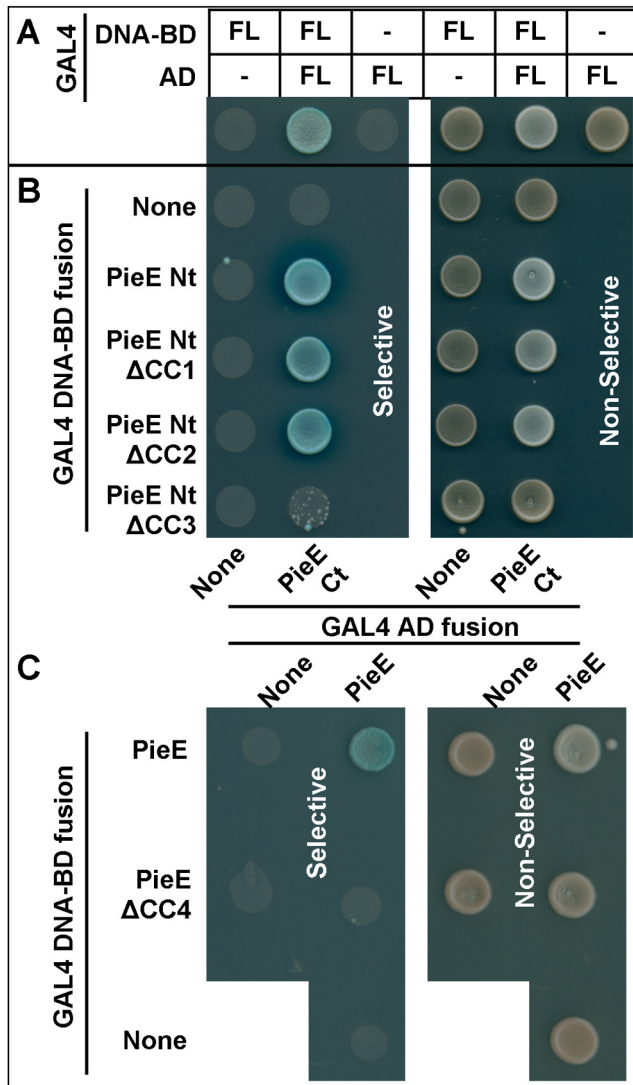
FIG 4 PieE dimerizes in a CC3- and CC4-dependent manner. *Saccharomyces cerevisiae* AH109 was cotransformed with plasmids allowing the coexpression of PieE (A) or the indicated PieE mutants (B and C) fused to GAL4 DNA-BD (bait) and the indicated PieE variants fused to GAL4 AD (prey), and growth on selective medium was monitored. FL, full length; Nt, N-terminal domain; Ct, C-terminal domain; PieE Nt ΔCC1, -2, -3, or -4, PieE N-terminal domain lacking the indicated CC region.

yeast β-galactosidase assay indicated that the interaction between PieE and the Rab GTPases might be weak (data not shown). By demonstrating that these interactions were mediated by CC1 and CC2, we defined a Rab GTPase-binding region in PieE (Fig. 7B). Recently, the crystal structure of the N-terminal domain of PpeA was reported (31). Although the homology of PieE and PpeA is too low for high-confidence modeling, overlay of the CC regions of PieE on the PpeA structure suggests that CC1 and CC2 might fold back on each other. This would result in a domain in which the loop between CC1 and CC2 forms the outermost tip of the protein and which is readily accessible for Rab GTPase interactions. In line with our results, deletion of either CC1 or CC2 would destroy this domain.

The effectors SidM, LepB, SidD, Lem3, LidA, and AnkX were previously shown to bind Rab1; RalF binds Arf1 and LidA binds several Rab GTPases (Rab1, -6a, and -8a) with very high affinity (13, 32, 33). We did not detect any of these effectors in the PieE complexes, suggesting that the interactions do not occur simultaneously or that the secondary interaction partners fall below the MS detection level.

Although PieE does not share structural similarity with LidA, both interact with several Rab GTPases. As PieE tethered rather than fused tubules of the ER, PieE might act, as proposed for LidA, as a tethering factor. In infection, PieE could promiscuously tether Rab GTPases and vesicles (Fig. 7B) or promote selective binding of some Rabs and repel or strip off others from vesicles, preventing fusion of undesired vesicles with the LCV. The observations that PpeA seems to interfere with endolysosome fusion (14) and trans-SNARE complex formation *in vitro* (34) might point to a vesicle filtering role for the PieE effector family.

Future work will uncover the role of the promiscuous interaction of PieE with Rab GTPases and the contribution of other proteins of the PieE interactome during *Legionella* infection. Importantly, the identification and validation of PieE interaction partners with proven relevance for *Legionella* infection demonstrate the power of our new TA purification method, which is widely applicable to other pathogens, host cells, or genetically tractable organisms, and show its potential to advance our understanding of the molecular mechanisms of infection.

MATERIALS AND METHODS

Bacteria, yeast, and eukaryotic cells. The culture of bacteria as well as maintenance and infection of eukaryotic cells was performed as described previously (16, 20). The strains used in this study are listed in Table S1A in the supplemental material. Transfection of HeLa or A549 cells with mammalian expression plasmids was performed using GeneJuice (Novagen) or Xfect (Clontech), respectively, according to the manufacturer's instructions. The A549 cell line stably expressing GFP-BirA was obtained by transfection with the pEGFP-BirA (pICC1394) plasmid, selection with 0.8 mg/ml G418 (Invitrogen), and subcloning. All yeast work was performed according to the Clontech yeast protocol handbook. For the Y2H spotting, overnight yeast cultures were adjusted to the same optical density at 600 nm (OD_{600}) by addition of fresh growth medium and 10 μl per sample was spotted on yeast solid medium.

Plasmid construction. Plasmids were constructed using standard molecular biology techniques with the primers and restriction enzymes described in Table S1B in the supplemental material. All the PieE constructs contained the PieE sequence from *L. pneumophila* 130b (ATCC BAA-74). Bioinformatic identification of PieE domains and motifs was carried out using SMART (35). Human Rab1a (hRab1a) was cloned using pCMV-SPORT6_hRab1a (MHS1010-57470) from Open Biosystems as the template, whereas the mouse Rabs (mRab1b, -2a, -5c, -6a, -7, and -10) were cloned using pENTR_Rabs as the template. The *birA* gene was amplified from the *E. coli* strain EDL933. The sequence identity and correct orientation of all inserts were verified by DNA sequencing.

Immunofluorescence microscopy. Cells on coverslips were fixed for 15 min with 4% formaldehyde, residual formaldehyde was quenched with 0.1 M glycine, and cells were permeabilized for 10 min at room temperature with 0.1% Triton X-100 or for 5 min at 4°C with 55 μg/ml digitonin. Phosphate-buffered saline (PBS) washes were carried out after each of these steps. After blocking in 5% fetal bovine serum, cells were sequentially incubated with primary and secondary antibodies diluted in 1% bovine serum albumin (BSA). Coverslips were mounted in ProLong Gold antifade reagent (Invitrogen) and analyzed using an Axio Observer.Z1 microscope (Carl Zeiss). Images were acquired and deconvoluted using AxioVision software (Carl Zeiss). The following primary antibodies were used at the indicated dilution: mouse anti-HA tag (Covance MMS-101P;
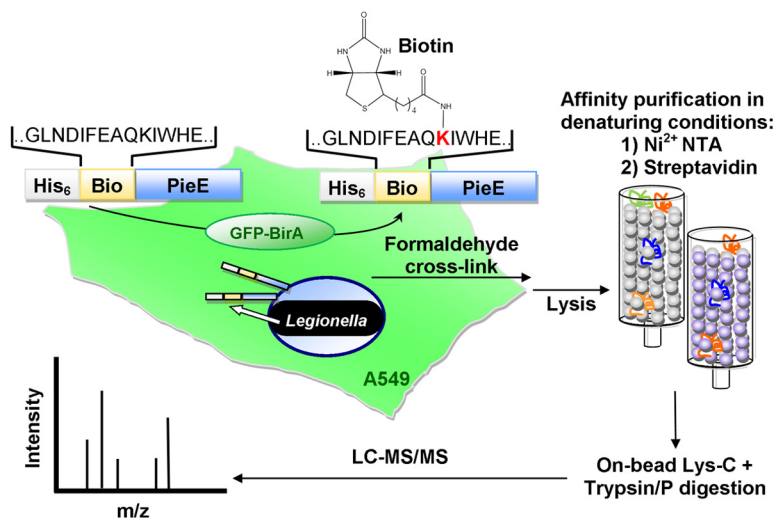
FIG 5 Scheme of the new TA purification method to determine the *in vivo* interactomes of effectors. An A549 cell line stably expressing the *E. coli* biotin ligase BirA (GFP-BirA) was infected with *L. pneumophila* 130b WT expressing PieE with an N-terminal TA purification tag, His$_6$-Bio, consisting of a hexahistidine tag and a specific BirA biotinylation sequence. After 19 h of infection, protein complexes were covalently cross-linked with formaldehyde, biotinylated effector complexes were isolated under denaturing conditions by a two-step affinity purification using Ni^{2+} chromatography and streptavidin chromatography, and samples were analyzed by LC-MS/MS.

1/500), mouse anti-Myc tag (Millipore 05-724; 1/500), rabbit anti-*L. pneumophila* (Affinity BioReagents PA1-7227; 1/800), rabbit antical-nexin (Stressgen SPA-860F; 1/100), and rabbit antigiantin (Abcam ab24586; 1/500). Secondary antibodies were obtained from Jackson Im-

munoResearch (1/200). Cellular and bacterial DNA was counterstained with Hoechst 33342.

Transmission electron microscopy. HeLa cells were washed 3 times with PBS and cooled on ice before fixation with 0.5% glutaraldehyde

TABLE 1 Host proteins specifically identified in the PieE sample after TA purification[c]

Protein	UniProt identifier	No. of unique peptides	Sequence coverage (%)	Biological function
SQSTM1/p62	Q13501	11	43	Regulation of various cell death and survival signaling pathways including selective autophagy
PABPC4	Q53GL4	8	15	Stabilization of mRNA and regulation of protein translation
RBM14/RBM4[a]	Q96PK6	8/2	15/8	Modulation of transcription
Rab1b	Q6FIG4	3	16	Regulation of vesicular traffic
NMP1	Q9BTI9	3	14	Roles in ribosome biogenesis, centrosome duplication, protein chaperoning, histone assembly, cell proliferation, and tumorigenesis
ATXN2L	Q8WWM7	4	6	Regulation of stress granules and processing bodies
Rab10	Q9UL28	3	21	Regulation of vesicular traffic
Calnexin	B4DGP8	3	6	ER-associated protein chaperone
Rab2a	P61019	3	20	Regulation of vesicular traffic
Rab1a	Q5U0I6	2	16	Regulation of vesicular traffic
Arf1 or 3[b]	P84077/P61204	2	14	Regulation of vesicular traffic
SCAMP3	Q6FHJ5	2	8	Carrier protein in post-Golgi vesicular recycling pathways
EIF5A	P63241	2	16	mRNA-binding protein involved in translation elongation
Rab7a	P51149	3	15	Regulation of vesicular traffic
TRIM4	Q9C037	3	7	Protein of unknown function
EIF4H	Q15056	2	11	Translation initiation factor involved in the initiation of protein synthesis
ZC3HAV1	Q7Z2W4	3	3	Induction of degradation of the viral mRNAs
Rab5c	P51148	2	12	Regulation of vesicular traffic
TFG	Q8TDJ5	2	3	Regulation of protein secretion at ER exit sites
Rab6a	P20340	2	11	Regulation of vesicular traffic

[a] Read-through transcription naturally occurs between the RBM14 and RBM4 genes. Both RBM14 and RBM4 were identified.

[b] Two peptides were identified that are both found in Arf1 and Arf3 and therefore do not allow discrimination.

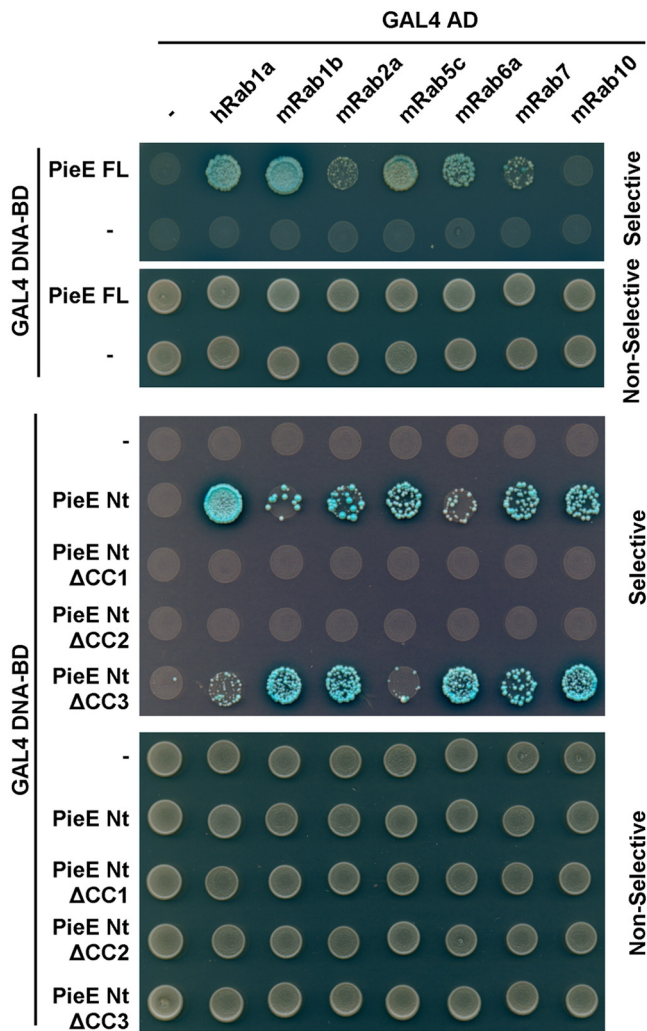[c] Order based on Mascot Percolator protein hit rank (PHR).

FIG 6 PieE contains a promiscuous Rab GTPase-binding domain. Direct Y2H assays using the indicated PieE bait and Rab GTPase prey plasmids showed that PieE directly interacts with the Rab GTPases 1a, 1b, 2a, 5c, 6a, 7, and 10 in a CC1- and CC2-dependent manner. hRab, human Rab GTPase; mRab, mouse Rab GTPase.

(Agar Scientific) in 200 mM sodium cacodylate (TAAB) for 5 min on ice and then at room temperature for a further 25 min. The cells were washed with 200 mM sodium cacodylate before postfixation in 1% osmium tetroxide-1.5% potassium ferrocyanide for 1 h. The cells were washed in double-distilled water (ddH$_2$O) and stained overnight at 4°C with 0.5% uranyl acetate. The cells were washed with ddH$_2$O before serial dehydration in graded ethanol. The cell monolayers were embedded flat in Epon 812 resin. Ultrathin sections (~70 nm) were cut parallel to the surface of the dish, collected onto Formvar-coated 50-mesh EM grids, and stained for 30 s with Reynolds' lead citrate before imaging.

Immunoelectron microscopy. Cells were fixed in 250 mM HEPES buffer, pH 7.4, containing 4% (wt/vol) paraformaldehyde for 10 min on ice and then at room temperature for a further 20 min. The cells were scraped from the dishes, pelleted by centrifugation, and fixed for a further 20 min in 250 mM HEPES buffer, pH 7.4, containing 8% (wt/vol) paraformaldehyde. Cell pellets were washed in PBS, frozen in 2.1 M sucrose-PBS, and stored under liquid nitrogen. Cryosections were prepared by the Tokuyasu method (36). Myc-PieE was detected using mouse monoclonal anti-Myc primary antibody (Millipore) diluted 1:50 in 5% fetal calf serum (FCS)-PBS, and ER was detected using mouse monoclonal anti-PDI antibody (a gift from M. Hollinshead, Section of Virology, Imperial College, London, United Kingdom). The mouse monoclonal antibodies were detected using rabbit anti-mouse antibody (diluted 1:50) and either 9-nm (Myc) or 6-nm (PDI) protein A-gold conjugates (gifted by M. Hollinshead).

Cryosections were also collected onto Xtra Adhesive glass microscopy slides (Leica) and immunofluorescently labeled for confocal microscopic analysis. Myc-PieE was detected using mouse monoclonal anti-Myc primary antibody diluted 1:500, and ER was detected using mouse monoclonal anti-PDI antibody diluted 1:10. The mouse monoclonal antibodies were detected using donkey anti-mouse Dylight 488 (Jackson ImmunoResearch), and nuclei were stained with DAPI (4[prime],6-diamidino-2-phenylindole).

Transmission electron microscopy and confocal microscopy were performed at the Henry Wellcome Imaging Centre, Division of Infectious Diseases, St. Mary's Hospital Campus, Imperial College, London, United Kingdom. TEM samples were viewed by using an FEI Tecnai G2 electron microscope with a Soft Imaging System Megaview III charge-coupled device camera. Images were collected at 1,376 by 1,032 by 16 pixels using AnalySIS version Docu software (Olympus Soft Imaging Solutions). Immunofluorescence images were acquired using a Zeiss LSM510 confocal microscope and processed using Adobe Photoshop (CS4).

Determination of *in vivo* interactomes of effectors. A 90% confluent monolayer of A549 cells, stably expressing GFP-BirA and grown in 150-cm² tissue culture dishes, was infected at a multiplicity of infection (MOI) of 50 for 19 h with post-exponential-growth-phase *L. pneumophila* 130b
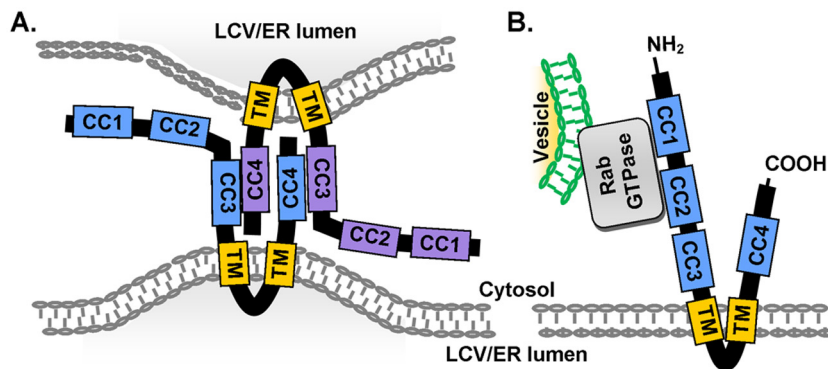

FIG 7 Models for the functional roles of the CC regions of PieE. (A) Two molecules of PieE in opposing membranes dimerize via CC3- and CC4-mediated interactions, stitching membranes together and facilitating intimate membrane contacts. (B) CC1 and CC2 of PieE mediate the interaction with Rab GTPases, controlling tethering and selective recruitment of vesicles to the LCV.

WT carrying the pICC1545 plasmid coding for His$_6$-Bio-PieE. The pICC1546 plasmid coding for His$_6$-Bio-LtpC or the empty vector pICC1544 was used as a control. The cell medium was supplemented with 6 μg/ml chloramphenicol, 1 mM IPTG (isopropyl-β-D-thiogalactopyranoside), and 4 μM D-biotin throughout the infection and was replaced after 2 h of infection. At the end of infection, cells were washed 3 times in PBS and protein complexes were cross-linked with 1% formaldehyde for 30 min at 37°C. Cross-linking was quenched with 125 mM glycine for at least 5 min at room temperature. Cells were then washed, and dry dishes were stored at −80°C. Infections were carried out with batches of 7 dishes per condition and repeated 6 times until 42 dishes per condition were obtained. Purification of protein complexes was performed at room temperature under denaturing conditions (adapted from the method in reference 19). Cells were scraped in lysis buffer (6 M guanidinium-HCl, 0.1 M Na$_2$HPO$_4$-NaH$_2$PO$_4$ [pH 8], 300 mM NaCl, 1% Triton X-100; pH 8; 5 ml per dish) and disrupted with one passage through an EmulsiFlex-B15 cell disruptor at 30,000 lb/in². Lysates were cleared by centrifugation for 20 min at 17,000 $\times$ *g*, and supernatants were incubated overnight with 1 ml of Ni-NTA agarose (Qiagen). The columns were then washed twice with wash buffer 1 (8 M urea, 0.1 M Na$_2$HPO$_4$-NaH$_2$PO$_4$ [pH 8], 300 mM NaCl, 1% Triton X-100, 20 mM imidazole; pH 8) and 5 times with wash buffer 2 (8 M urea, 0.1 M Na$_2$HPO$_4$-NaH$_2$PO$_4$ [pH 6.3], 300 mM NaCl, 1% Triton X-100, 20 mM imidazole; pH 6.3). The purified His$_6$-tagged proteins were then eluted with elution buffer N (8 M urea, 0.1 M Na$_2$HPO$_4$-NaH$_2$PO$_4$ [pH 4.5], 300 mM NaCl, 0.2% SDS, 250 mM imidazole; pH 4.3; 5 ml per column). The eluates were adjusted to pH 7.5 prior to incubation with 100-μl high-capacity streptavidin agarose (Pierce). The resin was sequentially washed 4 times with wash buffer 3 (8 M urea, 0.1 M Na$_2$HPO$_4$-NaH$_2$PO$_4$ [pH 7.5], 1 M NaCl, 0.2% SDS; pH 7.5) and once with wash buffer 4 (8 M urea, 0.1 M Na$_2$HPO$_4$-NaH$_2$PO$_4$ [pH 7.5], 1 M NaCl; pH 7.5).

For the LC-MS/MS analysis, the proteins on the streptavidin resin were reduced with 400 μl of 5 mM Tris(2-carboxyethyl)phosphine hydrochloride (TCEP; Sigma) and alkylated with 10 mM iodoacetamide (IAA; Sigma). Lys-C (1.5 μg; Roche) was added and incubated overnight at 25°C, and then 2.0 μg trypsin (Promega) was added to further digest for 6 h at 35°C and the supernatant was collected. Formic acid (FA) was added to the supernatant to a final concentration at 1% and 50 μl of 25% acetonitrile-0.1% FA to further extract peptides on the beads. The two eluted solutions were pooled and dried down in a SpeedVac (Thermo). The peptides were reconstituted with 0.1% FA-H$_2$O prior to mass spectrometric analysis.

The samples were analyzed with online nano-LC-MS/MS on an Ultimate 3000 capillary/nano-high-pressure liquid chromatography (HPLC) system (Dionex) coupled to an LTQ Orbitrap Velos hybrid mass spectrometer (Thermo Fisher) equipped with a nanospray source. Samples were first loaded and desalted on a PepMap C$_{18}$ trap (0.3 mm [inside diameter {i.d.}] by 5 mm; 5 μm; Dionex), and then peptides were separated on a 75-μm-i.d. by 10-cm BEH (ethylene bridged hybrid) C$_{18}$ column (1.7 μm; Waters) over a 60-min linear gradient of 4 to 32% CH$_3$CN-0.1% FA at a flow rate of 300 nl/min. The LTQ Orbitrap Velos mass spectrometer was operated in the "top 10" charge injection device (CID) data-dependent acquisition mode where the MS survey scan in the Orbitrap was *m/z* 380 to 160 with the lock mass at 445.120025 at a resolution of 60,000 at *m/z* 400. The automatic gain control (AGC) setting for Orbitrap is 1 $\times$ 10^6 with maximum injection time at 100 ms, and the MS/MS in the ion trap is 5,000 and 300 ms.

The raw files were processed with Proteome Discoverer 1.3 using the Mascot search engine (v2.3; Matrix Science) with the following parameters: trypsin/P with maximum 2 missed cleavage sites, peptide mass tolerance setting at first search of 10 ppm, and MS/MS fragment mass tolerance at 0.49 Da. Fixed modification for carbamidomethyl and variable modifications for acetyl (Protein N-term), deamidated (NQ), and oxidation (M) were used. The protein databases were combined with human IPI and *Legionella pneumophila* 130b.

The Mascot result files were further processed with in-house Mascot Percolator (http://www.sanger.ac.uk/resources/software/mascotpercolator/). The resultant proteins were filtered with a pairwise error probability (PEP) value of ≤0.01, which is equivalent to false discovery rates (FDRs) of less than 1%. Proteins with at least two unique peptides were reported (see Table S2 in the supplemental material). To obtain the list of proteins specifically isolated in the PieE complexes, proteins also identified in the Mascot Percolator results for either of the 2 control samples were first eliminated. In a second step, the data were also analyzed using MaxQuant (http://www.maxquant.org/) and proteins not identified with MaxQuant were removed from the list. The PRIDE partner repository (ProteomeXchange Consortium; http://proteomecentral.proteomexchange.org) accession numbers for the mass spectrometry proteomics data reported in this paper are PXD000706 and doi:10.6019/PXD000706.

SUPPLEMENTAL MATERIAL

Supplemental material for this article may be found at http://mbio.asm.org/lookup/suppl/doi:10.1128/mBio.01148-14/-/DCSupplemental.

Figure S1, TIFF file, 2.2 MB.
Figure S2, TIFF file, 2.3 MB.
Figure S3, TIF file, 3 MB.
Figure S4, TIFF file, 0.1 MB.
Figure S5, TIFF file, 7 MB.
Table S1, DOCX file, 0.1 MB.
Table S2, XLSX file, 0.4 MB.

REFERENCES

1. **Newton HJ, Ang DK, van Driel IR, Hartland EL.** 2010. Molecular pathogenesis of infections caused by *Legionella pneumophila*. Clin. Microbiol. Rev. **23:**274–298. http://dx.doi.org/10.1128/CMR.00052-09.

2. **Horwitz MA.** 1983. Formation of a novel phagosome by the Legionnaires' disease bacterium (*Legionella pneumophila*) in human monocytes J. Exp. Med. **158:**1319–1331. http://dx.doi.org/10.1084/jem.158.4.1319.

3. **Kagan JC, Roy CR.** 2002. *Legionella* phagosomes intercept vesicular traffic from endoplasmic reticulum exit sites. Nat. Cell Biol. **4:**945–954. http://dx.doi.org/10.1038/ncb883.

4. **Swanson MS, Isberg RR.** 1995. Association of *Legionella pneumophila* with the macrophage endoplasmic reticulum. Infect. Immun. **63:**3609–3620.

5. **Lifshitz Z, Burstein D, Peeri M, Zusman T, Schwartz K, Shuman HA, Pupko T, Segal G.** 2013. Computational modeling and experimental validation of the *Legionella* and *Coxiella* virulence-related type-IVB secretion signal. Proc. Natl. Acad. Sci. U. S. A. **110:**E707–E715. http://dx.doi.org/10.1073/PNAS1215278110.

6. **Segal G, Purcell M, Shuman HA.** 1998. Host cell killing and bacterial conjugation require overlapping sets of genes within a 22-kb region of the *Legionella pneumophila* genome. Proc. Natl. Acad. Sci. U. S. A. **95:**1669–1674. http://dx.doi.org/10.1073/pnas.95.4.1669.

7. **Vogel JP, Andrews HL, Wong SK, Isberg RR.** 1998. Conjugative transfer by the virulence system of *Legionella pneumophila*. Science **279:**873–876. http://dx.doi.org/10.1126/science.279.5352.873.

8. **Zhu W, Banga S, Tan Y, Zheng C, Stephenson R, Gately J, Luo ZQ.** 2011. Comprehensive identification of protein substrates of the Dot/Icm type IV transporter of *Legionella pneumophila*. PLoS One **6:**e17638. http://dx.doi.org/10.1371/journal.pone.0017638.

9. **Fontana MF, Banga S, Barry KC, Shen X, Tan Y, Luo ZQ, Vance RE.** 2011. Secreted bacterial effectors that inhibit host protein synthesis are critical for induction of the innate immune response to virulent *Legionella*

pneumophila. PLoS Pathog. **7**:e1001289. http://dx.doi.org/10.1371/journal.ppat.1001289.

10. **Ge J, Shao F.** 2011. Manipulation of host vesicular trafficking and innate immune defence by *Legionella* Dot/Icm effectors. Cell. Microbiol. **13**:1870–1880. http://dx.doi.org/10.1111/j.1462-5822.2011.01710.x.

11. **Rolando M, Sanulli S, Rusniok C, Gomez-Valero L, Bertholet C, Sahr T, Margueron R, Buchrieser C.** 2013. *Legionella pneumophila* effector RomA uniquely modifies host chromatin to repress gene expression and promote intracellular bacterial replication. Cell Host Microbe **13**:395–405. http://dx.doi.org/10.1016/j.chom.2013.03.004.

12. **Horenkamp FA, Mukherjee S, Alix E, Schauder CM, Hubber AM, Roy CR, Reinisch KM.** 2014. *Legionella pneumophila* subversion of host vesicular transport by SidC effector proteins. Traffic **15**:488–499. http://dx.doi.org/10.1111/tra.12158.

13. **Sherwood RK, Roy CR.** 2013. A Rab-centric perspective of bacterial pathogen-occupied vacuoles. Cell Host Microbe **14**:256–268. http://dx.doi.org/10.1016/j.chom.2013.08.010.

14. **de Felipe KS, Glover RT, Charpentier X, Anderson OR, Reyes M, Pericone CD, Shuman HA.** 2008. *Legionella* eukaryotic-like type IV substrates interfere with organelle trafficking. PLoS Pathog. **4**:e1000117. http://dx.doi.org/10.1371/journal.ppat.1000117.

15. **Ninio S, Celli J, Roy CR.** 2009. A *Legionella pneumophila* effector protein encoded in a region of genomic plasticity binds to Dot/Icm-modified vacuoles. PLoS Pathog. **5**:e1000278. http://dx.doi.org/10.1371/journal.ppat.1000278.

16. **Harding CR, Mattheis C, Mousnier A, Oates CV, Hartland EL, Frankel G, Schroeder GN.** 2013. LtpD is a novel *Legionella pneumophila* effector that binds phosphatidylinositol 3-phosphate and inositol monophosphatase IMPA1. Infect. Immun. **81**:4261–4270. http://dx.doi.org/10.1128/IAI.01054-13.

17. **Snapp EL, Hegde RS, Francolini M, Lombardo F, Colombo S, Pedrazzini E, Borgese N, Lippincott-Schwartz J.** 2003. Formation of stacked ER cisternae by low affinity protein interactions. J. Cell Biol. **163**:257–269. http://dx.doi.org/10.1083/jcb.200306020.

18. **Beckett D, Kovaleva E, Schatz PJ.** 1999. A minimal peptide substrate in biotin holoenzyme synthetase-catalyzed biotinylation. Protein Sci. **8**:921–929. http://dx.doi.org/10.1110/ps.8.4.921.

19. **Tagwerker C, Flick K, Cui M, Guerrero C, Dou Y, Auer B, Baldi P, Huang L, Kaiser P.** 2006. A tandem affinity tag for two-step purification under fully denaturing conditions: application in ubiquitin profiling and protein complex identification combined with in vivo cross-linking. Mol. Cell. Proteomics **5**:737–748. http://dx.doi.org/10.1074/mcp.M500368-MCP200.

20. **Schroeder GN, Petty NK, Mousnier A, Harding CR, Vogrin AJ, Wee B, Fry NK, Harrison TG, Newton HJ, Thomson NR, Beatson SA, Dougan G, Hartland EL, Frankel G.** 2010. *Legionella pneumophila* strain 130b possesses a unique combination of type IV secretion systems and novel Dot/Icm secretion system effector proteins. J. Bacteriol. **192**:6001–6016. http://dx.doi.org/10.1128/JB.00778-10.

21. **Witte K, Schuh AL, Hegermann J, Sarkeshik A, Mayers JR, Schwarze K, Yates JR, III, Eimer S, Audhya A.** 2011. TFG-1 function in protein secretion and oncogenesis. Nat. Cell Biol. **13**:550–558. http://dx.doi.org/10.1038/ncb2225.

22. **Aoh QL, Castle AM, Hubbard CH, Katsumata O, Castle JD.** 2009. SCAMP3 negatively regulates epidermal growth factor receptor degradation and promotes receptor recycling. Mol. Biol. Cell **20**:1816–1832. http://dx.doi.org/10.1091/mbc.E08-09-0894.

23. **Khweek AA, Caution K, Akhter A, Abdulrahman BA, Tazi M, Hassan H, Majumdar N, Doran A, Guirado E, Schlesinger LS, Shuman H, Amer AO.** 2013. A bacterial protein promotes the recognition of the *Legionella pneumophila* vacuole by autophagy. Eur. J. Immunol. **43**:1333–1344. http://dx.doi.org/10.1002/eji.201242835.

24. **Ohtsuka S, Ishii Y, Matsuyama M, Ano S, Morishima Y, Yanagawa T, Warabi E, Hizawa N.** 2014. SQSTM1/p62/A170 regulates the severity of *Legionella pneumophila* pneumonia by modulating inflammasome activity. Eur. J. Immunol. **44**:1084–1092. http://dx.doi.org/10.1002/eji.201344091.

25. **Tilney LG, Harb OS, Connelly PS, Robinson CG, Roy CR.** 2001. How the parasitic bacterium *Legionella pneumophila* modifies its phagosome and transforms it into rough ER: implications for conversion of plasma membrane to the ER membrane. J. Cell Sci. **114**:4637–4650.

26. **Belyi Y, Tabakova I, Stahl M, Aktories K.** 2008. Lgt: a family of cytotoxic glucosyltransferases produced by *Legionella pneumophila*. J. Bacteriol. **190**:3026–3035. http://dx.doi.org/10.1128/JB.01798-07.

27. **Shen X, Banga S, Liu Y, Xu L, Gao P, Shamovsky I, Nudler E, Luo ZQ.** 2009. Targeting eEF1A by a *Legionella pneumophila* effector leads to inhibition of protein synthesis and induction of host stress response. Cell. Microbiol. **11**:911–926. http://dx.doi.org/10.1111/j.1462-5822.2009.01301.x.

28. **Hoffmann C, Finsel I, Otto A, Pfaffinger G, Rothmeier E, Hecker M, Becher D, Hilbi H.** 2014. Functional analysis of novel Rab GTPases identified in the proteome of purified *Legionella*-containing vacuoles from macrophages. Cell. Microbiol. **16**:1034–1052. http://dx.doi.org/10.1111/cmi.12256.

29. **Shevchuk O, Batzilla C, Hägele S, Kusch H, Engelmann S, Hecker M, Haas A, Heuner K, Glöckner G, Steinert M.** 2009. Proteomic analysis of *Legionella*-containing phagosomes isolated from *Dictyostelium*. Int. J. Med. Microbiol. **299**:489–508. http://dx.doi.org/10.1016/j.ijmm.2009.03.006.

30. **Kubori T, Shinzawa N, Kanuka H, Nagai H.** 2010. *Legionella* metaeffector exploits host proteasome to temporally regulate cognate effector. PLoS Pathog. **6**:e1001216. http://dx.doi.org/10.1371/journal.ppat.1001216.

31. **Yao D, Cherney M, Cygler M.** 2014. Structure of the N-terminal domain of the effector protein LegC3 from *Legionella pneumophila*. Acta Crystallogr. D Biol. Crystallogr. **70**:436–441. http://dx.doi.org/10.1107/S139900471302991X.

32. **Machner MP, Isberg RR.** 2006. Targeting of host Rab GTPase function by the intravacuolar pathogen *Legionella pneumophila*. Dev. Cell **11**:47–56. http://dx.doi.org/10.1016/j.devcel.2006.05.013.

33. **Schoebel S, Cichy AL, Goody RS, Itzen A.** 2011. Protein LidA from Legionella is a Rab GTPase supereffector. Proc. Natl. Acad. Sci. U. S. A. **108**:17945–17950. http://dx.doi.org/10.1073/PNAS1113133108.

34. **Bennett TL, Kraft SM, Reaves BJ, Mima J, O'Brien KM, Starai VJ.** 2013. LegC3, an effector protein from *Legionella pneumophila*, inhibits homotypic yeast vacuole fusion *in vivo* and *in vitro*. PLoS One **8**:e56798. http://dx.doi.org/10.1371/journal.pone.0056798.

35. **Letunic I, Doerks T, Bork P.** 2012. SMART 7: recent updates to the protein domain annotation resource. Nucleic Acids Res. **40**:D302–D305. http://dx.doi.org/10.1093/nar/gkr931.

36. **Tokuyasu KT.** 1980. Immunochemistry on ultrathin frozen sections. Histochem. J. **12**:381–403. http://dx.doi.org/10.1007/BF01011956.